Surface Adsorption and Trapping of Xe on Hexagonal Ice at 180 K by Molecular Dynamics Simulations

S. Mitlin,[†] A. S. Lemak,[†] B. H. Torrie,[‡] and K. T. Leung*,[†]

Departments of Chemistry and Physics, University of Waterloo, Waterloo, Ontario N2L 3G1, Canada

Received: February 19, 2003; In Final Form: June 4, 2003

Classical molecular dynamics (MD) simulations of Xe on the basal (0001) face of hexagonal ice at 180 K have been performed in order to investigate the mechanism of adsorption and the initial stage of absorption of a van der Waals particle into crystalline ice. The potential of mean force (PMF) as a function of the relative position of the Xe atom perpendicular to the ice surface is found to increase abruptly as the particle propagates from the disordered outermost region to the deeper hexagonally ordered region. A set of local minima observed in the PMF appears to correspond directly to the layer-by-layer crystal structure of hexagonal ice. Along with the unbound state, the first two minima (with similar free energies) that correspond to the accommodation of the guest particle on and inside the disordered outermost bilayer, respectively, are found to be populated during the MD runs. The multiple transitions of the system among these three states are also observed in accord with the PMF profile, which also suggests that the penetration of any ordered hexagonal bilayer by the Xe atom is unlikely. Furthermore, MD simulations of pristine ice (i.e., without Xe) over a 3-ns simulation period show that the initially perfect-ordered hexagonal crystalline structure of the outermost bilayer undergoes transformation to a noncrystalline phase, in which fragmented domains with hexagonal ordering persist. Moreover, the accommodation of the Xe atom inside the outermost bilayer could facilitate further disordering of the hexagonal structure of this bilayer with the formation of a completely disordered Xe−ice surface phase.

1. Introduction

Molecular mechanisms of adsorption, trapping, penetration, and subsequent diffusion of different chemical species on ice are of fundamental importance to understanding a variety of physicochemical processes, including reactions of trace gases with ice and/or acid particles in the stratosphere and upper troposphere, interfacial chemistry on snowflakes, ice, and other water-covered particles in the biosphere, clathrate hydrates formation, and compositional evolution of ice particulates in interstellar space.[1−3] To date, both experimental and theoretical studies of the behavior of different chemical species on ice have not revealed a universal molecular mechanism for adsorption and absorption,[4] most likely because of an inherent complexity of the structure and the dynamics of the surface and the bulk of ice microphases. Of special interest is the adsorption and absorption behavior of an "inert" van der Waals (VdW) gas particle (such as Xe) on ice. In particular, Xe was reported to penetrate the ice structure to form clathrate hydrate experimentally first without an induction period by Pietrass et al.[5] but later with an induction period by Moudrakovski et al.[6] However, the mechanism concerning enclathration of Xe into the ice structure remains controversial. According to Sloan and Fleyfel, the formation of clathrate hydrate should be accompanied by considerable reconstruction of the ice lattice, which includes the formation of a surface liquid layer generated by mechanical action (surface agitation) on the ice sample.[7] On the other hand, Pietrass et al. have shown that Xe clathrate hydrate can be formed at a temperature as low as 195 K and a pressure of only 0.3 MPa and concluded the absence of a liquid water layer on ice.[5] Furthermore, Moudrakovski et al. have demonstrated that the kinetics of clathrate hydrate formation depends on the microcrystalline structure of ice, in which the average size of crystallites depends on the history of the sample.[6] In any event, guest species must penetrate the interface of the ice structure at a considerable depth (100−1000 Å) in order to form clathrate hydrates. It is obvious that the penetration of a noncrystalline medium should be easier and involves a different mechanism than the penetration of crystalline ice.[8] For example, Jenniskens and Blake have associated the anomalous gas retention and release from the "water-rich ices" above 150 K with the presence of noncrystalline microphases.[9] Given the early studies on this subject,[5−8,10] Xe therefore appears to be a useful probe for further exploring the adsorption and absorption mechanisms of a prototypical VdW particle on ice.

The penetration of the crystalline ice structure by "oversized" guest particles (with a VdW volume larger than the opening of a perfect water hexagon) is usually preceded by populating the adsorption sites. As it was demonstrated by Buch et al. for the CF_4/ice system[11] and by Kroes and Clary for the HCl/ice system,[12] there are at least two types of accessible adsorption states on the disordered surface of crystalline ice: those on and inside the disordered outermost bilayer. In the present work, we are adopting the same terminology by referring to the sites on and inside the disordered outermost bilayer as on-layer and in-layer adsorption states, respectively. However, as noted in the earlier studies,[11,12] the guest−ice interaction energy for the in-layer adsorption state is larger than that of the on-layer adsorption state. The existence of these two types of adsorption

* To whom correspondence should be addressed. E-mail: tong@uwaterloo.ca

[†] Department of Chemistry.

[‡] Department of Physics.

10.1021/jp034429z CCC: $25.00
Published on Web 08/22/2003

states was also demonstrated by Girardet and Toubin in the MD simulations of HCl and HOCl on ice at 200 K.[4] Further penetration of the guest particles into the bulk was found to be accompanied by a significant increase in the free energy of the system,[4] which is most likely caused by partial disruption of an initially perfectly ordered hydrogen-bonded structure of the second and inner bilayers. The energies and structural parameters of the adsorption states should depend on the equilibrium organization of the outermost bilayer of the ice surface, which inherently assumes that the temperature of the guest/ice system is an important parameter for the adsorption and absorption mechanisms. On the other hand, using a short (3 ps) MD simulation, Al-Halabi et al.[13,14] showed that for 110−190 K hyperthermal HCl molecules with energies exceeding 100 kJ/mol could either adsorb on or directly penetrate the ideal (0001) hexagonal surface through the openings of surface hexagons, leading to the absorption of the guest particle at an interstitial site between the water bilayers.

Of relevance to atmospheric chemistry is the temperature range of 180−270 K, over which surface melting of ice occurs with disordering of the outermost bilayer and then proceeds further in depth with the formation of a quasi-liquid layer at the higher temperature end (i.e., near 270 K).[4,15] In particular, MD studies of the surface dynamics of TIP4P ice Ih by Bolton and Pettersson showed that already at 180 K the equilibrium organization of the outermost bilayer is noncrystalline with the emergence of different surface polygons (from pentagons to octagons) in dynamical coexistence,[16] which is in accord with the early results of Kroes at 190 K.[17] Bolton and Pettersson further demonstrated that in the case of Ar impinging on ice the dynamics of the ice surface is responsible for the reversible adsorption-trapping-desorption cycle.[18] In particular, Ar was found to penetrate the disordered outermost bilayer quickly, visiting for a relatively short time (with an average lifetime of 120 ps) the absorption sites in the heptagon and octagon structures before leaving the ice surface.[18] This study has in effect suggested that Ar atoms cannot penetrate the ordered second bilayer of the crystalline ice structure.[18] On the other hand, the enclathration of Ar into ice was observed experimentally by Hallbrucker and Mayer[19] at 200 K and 1 bar, at which conditions the formation of a quasi-liquid surface layer is not expected. It should be noted that the process of direct penetration of the hyperthermal particle described by Al-Halabi et al.,[13,14] in which dynamic rearrangement of the surface water hexagons plays little or no role, should be distinguished from that of trapping into the disordered outermost bilayer predicted by Buch et al.,[11] Kroes and Clary,[12] and Bolton and Pettersson.[18] These studies raise further questions about the absorption and trapping mechanisms of a VdW particle in crystalline ice. In the present work, we investigate the details of these fundamental surface processes on crystalline ice at 180 K by classical MD simulations using Xe as the probe atom.

2. Methods and Computational Details

MD simulations of a Xe atom on the basal (0001) plane of a proton-disordered hexagonal ice slab were performed using the CHARMM program[20] employing the TIP4P model for the water molecules.[21] The VdW interactions between any pair of the nonbonded atoms for the Xe−Xe and Xe−H_2O systems were described by the Lennard-Jones (12,6) potential (LJ). The CHARMM program uses the arithmetic-mean combining rule for the Rmin_{ij} ($\mathrm{Rmin}_{ij} = 1/2[\mathrm{Rmin}_{ii} + \mathrm{Rmin}_{jj}]$) LJ parameters and the geometric-mean combining rule for the ϵ_{ij} ($\epsilon_{ij} = [\epsilon_{ii} \cdot \epsilon_{jj}]^{1/2}$) LJ parameters.[20] The LJ parameters for the Xe−Xe VdW interaction were adopted from Tanaka[22] with the following values for $\epsilon_{\mathrm{XeXe}} = -0.4591$ kcal/mol and $\mathrm{Rmin}_{\mathrm{XeXe}} = 4.5426$ Å. The LJ parameters for the VdW interactions for the Xe−O and Xe−H pairs are as follows: $\epsilon_{\mathrm{XeO}} = -0.27026$ kcal/mol and $\mathrm{Rmin}_{\mathrm{XeO}} = 3.8712$ Å and $\epsilon_{\mathrm{XeH}} = -0.15121$ kcal/mol and $\mathrm{Rmin}_{\mathrm{XeH}} = 3.0714$ Å.

Periodic boundary conditions were imposed in the x and y directions of the basal surface of ice such that the rectangular MD simulation box with (x, y) size of (26.945 Å, 31.113 Å) contains one Xe atom and an ice slab made up of 8 bilayers with 96 water molecules in each bilayer. To preserve the crystallinity of the ice structure, the four bottom bilayers (i.e., the 5th to 8th bilayers) were kept rigid during the simulations. The initial coordinates of the water molecules in the ice slab were obtained from Buch et al.[23]

MD trajectories were generated using the leapfrog integrator with 1 fs integration step at a constant temperature of 180 K. The SHAKE algorithm was employed for keeping the water molecules rigid by constraining the distances between the atoms in a molecule.[24] The cutoff distance for nonbonded interactions was set to 13 Å in order to be consistent with the simulation box size.

The free energy change can be obtained by calculating the potential of mean force (PMF).[25] In particular, the PMF as a function of z coordinate of the Xe atom (along the perpendicular direction to the ice surface), $W(z)$, was obtained by carrying out the umbrella sampling,[26] where the potential energy of the Xe−ice system was changed by applying an umbrella potential $V_s(z) = k_s(z - z_s)^2$ to the Xe atom in order to restrict the sampling range of z in a given run around a prescribed z_s value. Sixty separated MD runs were performed using a series of different z_s values chosen for each simulation, so that successive simulations sample overlapping regions in the range 17.5 Å < z < 32.5 Å. The force constants k_s in the umbrella potential were set to 5.2516 and 2.6258 kcal/(mol Å^2) in the simulations where the motion of the Xe atom was restricted outside and inside the ice, respectively. The first simulation run was started with the ideal hexagonal crystalline structure of ice (obtained from Buch et al.[23]), whereas the starting configuration for each subsequent run was taken from the previous one. For each run, the MD trajectory over a 150 ps period was collected for further analysis. The WHAM technique[27] adopted from Lemak and Gunn[28] was employed for calculating in a canonical ensemble the probability distribution of z coordinate of Xe, $P(z)$, which could in turn be used to determine the PMF according to the relation $W(z) = -k_B T \ln P(z)$ (where k_B is the Boltzmann constant).

To study the surface dynamics of Xe, the MD simulations have been extended to 1, 2, and 4 Xe atoms on the ice surface without applying an umbrella potential to the system at a constant temperature of 180 K. With the Xe atoms initially located randomly at the on-layer adsorption site ϵ_1 (and at $z \sim$ 29 Å), the MD trajectories were propagated for a 3 ns period.

Structural evolution of the ice surface has been followed by observing the order parameter, which is an average of three translational order parameters introduced by Kroes,[17] along the MD trajectories for the ice and Xe−ice systems. This order parameter S_T equals 1 for perfectly ordered hexagonal lattice, whereas it is of the order $1/N$ ($\sim$0.02) for a structure without hexagonal order, where $N = 48$ is the number of water molecules in a half bilayer of ice structure in the simulation box.

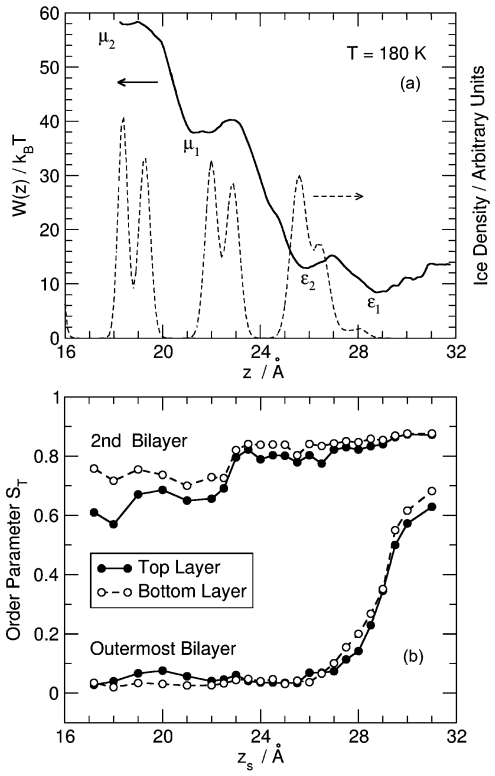

Figure 1. (a) Potential of mean force, $W(z)$, as a function of the z-coordinate for the Xe−ice system at 180 K. The broken lines show the relative density profile of the oxygen atoms for a pristine ice lattice. The two adsorption sites outside the ice surface and inside the outermost bilayer and the two absorption sites inside the ice slab are labeled by ϵ_1, ϵ_2, μ_1, and μ_2, respectively. (b) Translational order parameter S_T for the top (solid circles) and bottom (open circles) layers of the outermost and second outermost bilayers of the ice slab as a function of z_s, the constrained position of the Xe atom in the series of umbrella sampling simulations. The lines are drawn for eye guidance only.

3. Results and Discussion

3.1. Potential of Mean Force of Xe on Ice. The PMF for the Xe−ice system along the z direction shown in Figure 1a exhibits a set of minima of increasing free energy values at positions closely associated with the layer-by-layer structure of hexagonal ice. In particular, the minimum located outside the ice structure on the surface corresponds to the on-layer adsorption state ϵ_1 of the Xe atom. Existence of this minimum with respect to an unbound state is due to VdW attraction of Xe to ice, the outermost bilayer of which is a disordered and heterogeneous structure. The next local minimum is located inside the first disordered bilayer and it corresponds to the in-layer adsorption state ϵ_2. The existence of a continuous open path from the unbound state to the ϵ_2 state justifies its designation as an adsorption state. The subsequent local PMF minima localized inside the ice structure are identified as a set of Xe absorption states $\{\mu_i\}$. The sharp increase in free energy between subsequent absorption states is associated with partial disruption of the crystalline structure of the corresponding bilayer. Local disruption of the bilayer is necessary for the accommodation of the Xe atom because the VdW volume of Xe is larger than the free space available in the ideal hexagonal ice lattice. For example, transition of the system from the in-layer adsorption state ϵ_2 to the first absorption state μ_1 is accompanied by an increase in free energy of 9 kcal/mol (Figure 1a) and local disruption of the initially ordered second bilayer. Evidently, this transition also causes a decrease in the translational order parameters S_T for the second bilayer shown in Figure 1b. In contrast to the transition to the first absorption state and between absorption states of higher order, there is a relatively small free energy difference (∼1.8 kcal/mol) between the two adsorption states ϵ_1 and ϵ_2, which are separated only by a small barrier (Figure 1a). Low degree of crystallinity of the outermost bilayer (Figure 1b) is therefore responsible for the PMF profile in this spatial region (Figure 1a). The significantly larger change in the free energy accompanying the $\epsilon_2 \rightarrow \mu_1$ transition relative to that of the $\epsilon_1 \rightarrow \epsilon_2$ transition is consistent with the much higher degree of ordering of the second bilayer relative to the first (outermost) bilayer (Figure 1b).

The PMF profile of the Xe−ice system at 180 K (Figure 1a) appears to be qualitatively similar to the free energy profiles of HCl and HOCl on hexagonal ice at 200 K reported by Girardet and Toubin (see Figure 18 in Ref 4). Although the VdW sizes of these molecules and Xe are larger than the opening of the hexagon of water molecules, the observed similarity in the PMF profiles is unexpected because the interactions of HCl and HOCl with ice include the strong electrostatic potential in addition to the VdW potential. There are, however, notable quantitative differences between these systems. In particular, the free energy change for the $\epsilon_2 \rightarrow \mu_1$ transition for the Xe−ice system at 180 K is about twice that for the HCl−ice and HOCl−ice systems at 200 K, which may be attributed either to a decrease in the activation energy of structural reconstruction of ice due to electrostatic interaction or to an increase in the degree of disorder of the second bilayer with increasing temperature. It is also noteworthy that the PMF profiles for guest−ice systems considered in the present work and by Girardet and Toubin[4] represent the resistance of the ice structure against the disruption introduced by the guest particle penetration. Moreover, the similarities in the PMF profiles suggest that intermolecular interactions in the ice structure itself appear to be more important, at least at a qualitative level, for the determination of the PMF profile than a specific guest-ice interaction.

Finally, the present PMF profile for the Xe−ice system (Figure 1a) clearly shows that at 180 K there are relatively large probabilities of occupying an unbound state and the adsorption states (ϵ_1 and ϵ_2) of the Xe atom, whereas those of occupying μ_1 and higher-order absorption states (such as μ_2) are very small. These results are connected to the order−disorder equilibrium in the ice surface and the near-surface region.

3.2. Order−Disorder of the Xe−Ice Surface. Earlier experimental and theoretical studies of the surface properties of ice[4,15−17,29,30] suggested that an equilibrium state of the pristine hexagonal ice surface below 170 K is dominated by a hexagonally ordered crystalline structure, whereas for 180−220 K, it most likely involves significant disorder in the outermost bilayer but with nearly perfect crystalline organization for the inner bilayers. In particular, Nada and Furukawa[15] concluded from their MD simulations of TIP4P hexagonal ice that the relaxation time for this system at 185 K is less than 1 ns, within which the outermost bilayer is found to evolve into a disordered structure. Such a disordered structure is characterized by the presence of water admolecules that "jump out" from the outermost bilayer.[15] In addition, over the MD simulation time of tens of nanoseconds at temperatures above 180 K, Bolton and Pettersson[16] have observed interbilayer migration of water molecules with preferential motion into the inner layers, which leads to the appearance of nonzero density between the first and second outermost bilayers and an increase in the number of molecules in the second bilayer. However, it should be noted that there is no direct correspondence between the temperature used in the MD simulations and the experimental temperature

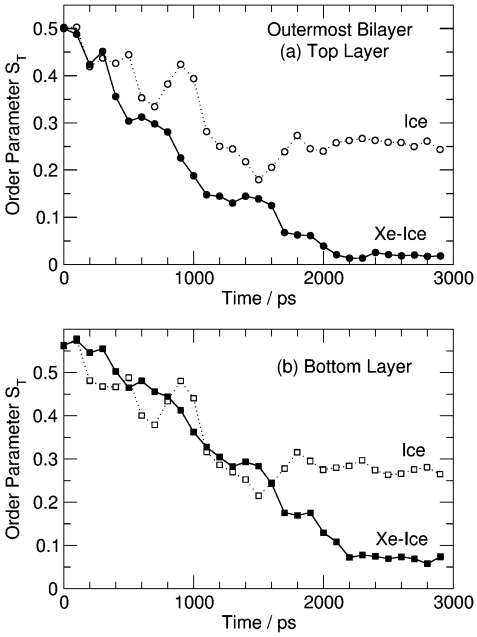

Figure 2. Translational order parameter S_T of (a) the top and (b) bottom layers of the outermost bilayer as a function of simulation time for two MD trajectories started from the same ice configuration. Open and solid symbols correspond to the trajectories of pristine ice and Xe−ice systems, respectively. Each point represents the S_T value averaged over 100 ps.

because, for instance, the melting point of a proton-ordered TIP4P hexagonal ice was calculated by Volt et al. to be ∼214 K at 1 atm,[31] which is significantly lower than the experimentally observed value of 273 K.

In the present study, the translational order parameter S_T for pristine hexagonal ice at 180 K was monitored over a period of 3 ns along a MD trajectory started from a nonequilibrium configuration. In particular, S_T for both the top and bottom layers of the outermost bilayer are found to decrease from an initial value of ∼0.5 and level off near 0.3 after 1 ns (Figure 2), which indicates the onset of a long-lived state of ice having a partially disordered first bilayer. Although molecules primarily from the top bilayer were occasionally observed in the interlayer region, no density in this region is found in the molecular density profile of ice shown in Figure 1a, which is consistent with the lack of significant interbilayer migration in this long-lived state. Figure 3a shows a typical configuration of the oxygen atoms of the water molecules in the first bilayer in this stable state, which evidently consists of a few admolecules and a set of different polygons formed by 5, 6, and 7 water molecules. The existence of admolecules also manifests itself as a shoulder near 28 Å in the density profile (Figure 1a), which is in agreement with the calculations by Nada and Furukawa.[15] A similar polygonal noncrystalline structure for the top bilayer of ice at 180 K was also reported by Bolton and Pettersson.[16,18] It should be noted that, despite a significant overall disorder in the first bilayer, there are regions on the ice surface where the nearly perfect hexagonal structure is preserved (Figure 3a, lower right). The structural organization of the outermost bilayer of hexagonal ice at 180 K as revealed by the present MD simulations is therefore characterized by the coexistence of dynamical polygons, slightly distorted hexagonal fragments, admolecules, and occasional interbilayer water molecules. This structure exhibits uneven local distribution of molecular density inside the bilayer, and the areas of rarefied density provide the openings for guest particle trapping in the ϵ_2 adsorption state.

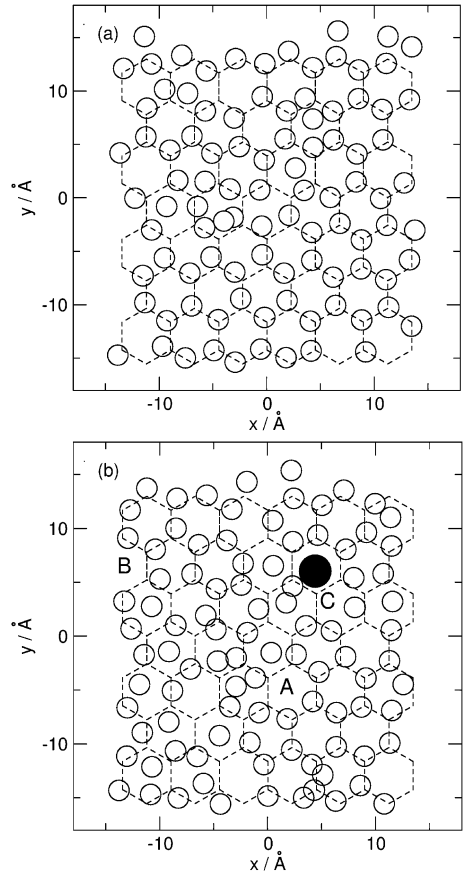

Figure 3. Snapshot of the positions of oxygen atoms in the outermost bilayer (open circles) for $t = 3$ ns on a typical trajectory of (a) the pristine ice surface and (b) the Xe−ice system. The position of the Xe atom is shown as a solid circle. The positions A, B, and C correspond to the ϵ_2 adsorption sites in the outermost bilayer visited by the Xe atom. The oxygen positions of the ideal hexagonal ice structure are represented by the junction points of the honeycomb grid drawn with dashed lines in (a and b).

The present MD simulations show that the presence of a Xe atom on the ice surface promotes further disordering of the outermost bilayer and increases the number of molecules appearing between the first and second bilayers. As shown in Figure 2, the S_T parameters for the Xe−ice system are found to level off at 0.025 and 0.05 for the top and bottom layers, respectively. These S_T values are therefore notably smaller than the corresponding S_T values of 0.3 for the pristine ice system (Figure 2), indicating the formation of a long-lived disordered state for the Xe−ice system with a substantially lower concentration of hexagonally ordered fragments. Indeed, the snapshot of the outermost bilayer for the Xe−ice system (Figure 3b) clearly demonstrates the noticeably more disordering of the outermost bilayer relative to that for the pristine ice system (Figure 3a). Kinetically, the disordering process in the outermost bilayer is found to proceed at a higher rate at those moments when the Xe atom is located in the in-layer adsorption state ϵ_2. It should be noted that the corresponding water density profile of the Xe−ice system is found to be nearly identical to that of the pristine ice system (Figure 1a). However, the presence of Xe in the ϵ_2 state enhances molecular motion in the interbilayer region of the ice lattice with barely discernible density between the first and second bilayers. The formation of the Xe-containing phase on the ice slab surface is therefore not only much more laterally disordered from the hexagonal arrangement but also more diffuse in the z direction relative to the outermost bilayer of pristine ice at 180 K. In effect, the Xe−ice phase formation

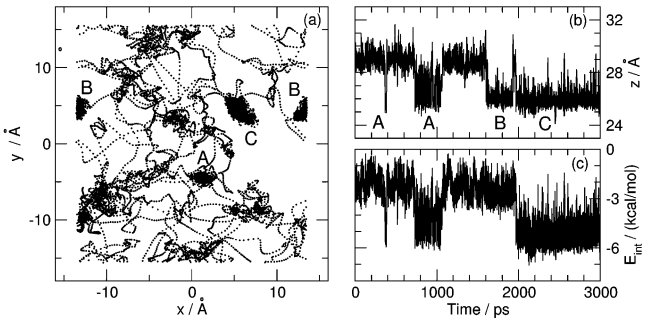

Figure 4. Typical trajectory of the Xe atom on the ice surface (a) in the (*x*, *y*) plane and (b) along the corresponding z-coordinate of the Xe atom. The positions A, B, and C correspond to the ϵ_2 adsorption sites in the outermost bilayer visited by Xe atom. (c) Interaction energy (E_{int}) of Xe atom with the ice slab as a function of time for the same trajectory.

causes partial "fluidization" of the surface of the ice slab by facilitating a more fluidlike outermost bilayer, which is in accord with the model introduced by Molina.[32] In contrast to the Xe−ice system, the MD simulations of HCl adsorption on a 18 Å-thick Ih ice film supported by MgO at 190 K by Toubin et al.[33] have demonstrated that ordering of the outermost bilayer persists for the HCl adsorption and absorption processes at a coverage of 0.3 monolayer with a slight increase in the S_T parameter from 0.4 to 0.5. Similar S_T values for different HCl−ice adsorption/absorption complexes obtained by MD simulations were also reported by Kroes and Clary[12] and by Gertner and Hynes.[34] At higher HCl coverages of 0.6 and 1.0 monolayer, the S_T parameters for the outermost bilayer were found to decrease to the level of 0.2 and 0.1, respectively,[33] which are still higher than that of the Xe−ice system after 2 ns of simulation. This notable difference in the S_T parameters for the Xe−ice and HCl−ice systems could be attributed to the effect of an electrostatic component of HCl−ice interaction. In particular, the presence of the hydrogen bonding between HCl and surface water molecules theoretically shown by Kroes and Clary[12] could account for the preservation of partial ordering of the ice surface.

3.3. Surface Dynamics of Xe. To illustrate the details of the molecular mechanism in populating the ϵ_1 and ϵ_2 adsorption states by the guest particle, the dynamics of 1, 2, and 4 Xe atoms on the ice surface at 180 K has been followed by MD simulation over a period of 3 ns.[35] In particular, the Xe atom impinging on a disordered ice surface is found to be accommodated either in the ϵ_1 state or directly in the ϵ_2 state, the latter of which is possible if the guest particle accidentally enters the openings in the outermost bilayer (Figure 3). Figure 4a shows a typical trajectory of a single Xe atom on the ice surface. Evidently, starting initially in the ϵ_1 state, the Xe atom has repeatedly visited the ϵ_2 state, penetrating the outermost disordered bilayer and being trapped at different locations (A, B, and C), before finally accommodated in the ϵ_2 state for more than 1 ns (Figure 4b). In the ϵ_1 state, the Xe atom has high lateral mobility (Figure 4a), which allows it to probe an ensemble of dynamic polygons of different sizes and shapes and indeed to penetrate into, where appropriate, the accessible opening. In contrast, the ϵ_2 adsorption state is characterized by its limited lateral mobility, which constrains the Xe atom to a polygon site.

Figure 4c shows the corresponding interaction energy of Xe−ice along the same trajectory shown in Figure 4a. Evidently, the interaction energy for the ϵ_2 state appears to be larger by 2−3 kcal/mol than that for the ϵ_1 state for positions A and C but remains unchanged for position B. The energy difference between B and C is caused by different specific configurations of the water molecules surrounding the Xe atom. In position C, the Xe atom is located directly above the center of the water hexagon of the second bilayer and is tightly surrounded by 10 water molecules of the first bilayer. On the other hand, the Xe atom at position B is found to be atop of a water molecule from the second bilayer with a loosely bound neighborhood in the first bilayer. For the ϵ_2 adsorption state, the preferred trapping site for the Xe atom therefore includes the center of the hexagon of the second bilayer. The dynamics of a single Xe atom on the ice surface is similar to that observed for Ar by Bolton and Pettersson[18] with the important difference that the characteristic occupancy times of the ϵ_1 and ϵ_2 states for the Xe atom (over 1 ns) are an order of magnitude greater than that for the Ar atom (120 ps).

MD simulations of 2 and 4 Xe atoms on the ice surface demonstrate reversible transitions of Xe atoms between three states: (a) unbound (gaseous) state, (b) on-layer adsorption state ϵ_1, and (c) in-layer adsorption state ϵ_2 on a time scale of 3 ns. The interaction among Xe atoms gives rise to interesting dynamical phenomena, including the formation of weakly bound pairs of Xe atoms (Xe dimers) in both the ϵ_1 and ϵ_2 states and fast exchange of Xe atoms in these states. Break up of the Xe dimers could result in desorption of individual Xe atoms from the surface. These results will be presented in a follow-up paper.[35] The dynamics of the system observed in these simulations[35] is in good accord with the PMF for Xe−ice system represented in Figure 1a.

4. Concluding Remarks

In the present work, we show that the PMF can be used to illustrate the degree of disruption of the crystalline structure of the ice lattice, which is required to accommodate a guest species, even though the specific nature of the guest−ice interaction appears to be less important to the qualitative features of the free energy profile. In good accord with the PMF profile, the dynamics of the Xe−ice system demonstrates several fundamental surface processes, including Xe adsorption on the ice surface, Xe trapping into various polygon sites of the outermost bilayer, and transitions between these states. The presence of Xe atom in the in-layer adsorption state is found to be remarkably effective in introducing disorder in the outermost bilayer.

Acknowledgment. This work is supported by the Natural Sciences and Engineering Research Council of Canada. It is our pleasure to acknowledge Professor V. Buch (Hebrew University of Jerusalem) for providing us with the coordinates of the ideal proton-disordered ice structure.

References and Notes

(1) Domine, F.; Shepson, P. B. *Science* **2002**, *297*, 1506.
(2) Zondlo, M. A.; Hudson, P. K.; Prenni, A. J.; Tolbert, M. A. *Annu. Rev. Phys. Chem.* **2000**, *51*, 473.
(3) Kouchi, A.; Yamamoto, T. *Prog. Cryst. Growth Charact.* **1995**, 30, 83.
(4) Girardet, C.; Toubin, C. *Surf. Sci. Rep*. **2001**, *44*, 159.
(5) Pietrass, T.; Gaede, H. C.; Bifone, A.; Ripmeester, J. A. *J. Am. Chem. Soc*. **1995**, *117*, 7520.
(6) Moudarkovski, I. L.; Sanchez, A. A.; Ratcliffe, C. I.; Ripmeester, J. A. *J. Phys. Chem. B* **2001**, *105*, 12338.
(7) Sloan, E. D.; Fleyfel, F., Jr. *AIChE J.* **1991**, *37*, 1281.
(8) Laufer, D.; Kochavi, E.; Bar-Nun, A. *Phys. Rev. B* **1987**, *36*, 9219.
(9) Jenniskens, P.; Blake, D. F. *Science* **1994**, *265*, 753.
(10) Notesco, G.; Laufer, D.; Bar-Nun, A.; Owen, T. *Icarus* **1999**, *142*, 298.

(11) Buch, V.; Delzeit, L.; Blackledge, C.; Devlin, J. P. *J. Phys. Chem*. **1996**, *100*, 3732.
(12) Kroes, G.-J.; Clary, D. C. *J. Phys. Chem*. **1992**, *96*, 7079.
(13) Al-Halabi, A.; Klein, A. W.; Kroes, G.-J. *J. Chem. Phys*. **2001**, *115*, 482.
(14) Al-Halabi, A.; Klein, A. W.; Kroes, G.-J. *Chem. Phys. Lett*. **1999**, *307*, 505.
(15) Nada, H.; Furukawa, Y. *Surf. Sci*. **2000**, *446*, 1.
(16) Bolton, K.; Pettersson, J. B. C. *J. Phys. Chem. B* **2000**, *104*, 1590.
(17) Kroes, G.-J. *Surf. Sci*. **1992**, *275*, 365.
(18) Bolton, K.; Pettersson, J. B. C. *Chem. Phys. Lett*. **1999**, *312*, 71.
(19) Hallbrucker, A.; Mayer, E. *J. Chem. Soc., Faraday Trans*. **1990**, *86*, 3785.
(20) Brooks, B. P.; Bruccoleri, P. E.; Olafson, B. D.; States, D. J.; Swaminathan, S.; Karplus, M. *J. Comput. Chem*. **1983**, *4*, 187.
(21) Jorgensen, W. L.; Chandrasekhar, J.; Madura, J. F.; Impley, R. W.; Klein, M. L. *J. Chem. Phys.* **1983**, *79*, 926.
(22) Tanaka, H. *Fluid Phase Equilib.* **1998**, *144*, 361.
(23) Buch, V.; Sandler, P.; Sadlej, J. *J. Phys. Chem. B* **1998**, *102*, 8641.
(24) Ryckaert, J. P.; Ciccotti, G.; Berendsen, H. J. C. *J. Comput. Phys*. **1977**, *23*, 327.
(25) McQuarrie, D. A. *Statistical Mechanics*; Harper and Row: New York, 1976.
(26) Torrie, G. M.; Valleau, J. P. *J. Comput. Phys*. **1977**, *23*, 187.
(27) Kumar, S.; Bouzida, D.; Swendsen, R. H.; Kollman, P. A.; Rosenberg, J. M. *J. Comput. Chem*. **1992**, *13*, 1011.
(28) Lemak, A. S.; Gunn, J. R. *J. Phys. Chem. B* **2000**, *104*, 1097.
(29) Materer, N.; Starke, U.; Barbieri, A.; Van Hove, M. A.; Somorjai, G. A.; Kroes, G.-J.; Minot, C. *Surf. Sci*. **1997**, *381*, 190.
(30) Geiger, F. M.; Tridico, A. C.; Hicks, J. M. *J. Phys. Chem. B* **1999**, *103*, 8205.
(31) Volt, M. J.; Huinik, J.; van der Eerden, J. P. *J. Chem. Phys*. **1999**, *110*, 55.
(32) Molina, M. J. *The Chemistry of the Atmosphere: Its Impact on Global Change*; Blackwell Scientific, Oxford, 1994; p 27−38.
(33) Toubin, C.; Picaud, S.; Hoang, P. N. M.; Girardet, C.; Demirdjian, B.; Ferry, D.; Suzanne, J. *J. Chem. Phys*. **2002**, *116*, 5150.
(34) Gertner, B. J.; Hynes, J. T. *Faraday Discus*. **1998**, *110*, 301.
(35) Mitlin, S.; Lemak, A. S.; Leung, K. T. to be published.